REPORT DOCUMENTATION PAGE

Form Approved
OMB No. 0704-0188

1. REPORT DATE *(DD-MM-YYYY)*	2. REPORT TYPE	3. DATES COVERED *(From - To)*
30-12-2003	Final	01-06-1998/31-12-2003

4. TITLE AND SUBTITLE
Electrophotographic Solid Freeform Fabrication.

5a. CONTRACT NUMBER

5b. GRANT NUMBER
N00014-98-1-0694

5c. PROGRAM ELEMENT NUMBER

6. AUTHOR(S)
Ashok Kumar

5d. PROJECT NUMBER

5e. TASK NUMBER

5f. WORK UNIT NUMBER

7. PERFORMING ORGANIZATION NAME(S) AND ADDRESS(ES)

University of Florida
Mechanical and Aerospace
Engineering
231 Aerospace Building
Gainesville FL 32611-6250

8. PERFORMING ORGANIZATION REPORT NUMBER

9. SPONSORING / MONITORING AGENCY NAME(S) AND ADDRESS(ES)
Office of Naval Research
Regional Office Atlanta
100 Alabama Street SW
Suite 4R15
Atlanta, GA 30303-3104

10. SPONSOR/MONITOR'S ACRONYM(S)

11. SPONSOR/MONITOR'S REPORT NUMBER(S)

12. DISTRIBUTION / AVAILABILITY STATEMENT

Approved for Public Release; distribution is unlimited

13. SUPPLEMENTARY NOTES

14. ABSTRACT

A method for solid freeform fabrication based on electrophotographic powder deposition was investigated to study its potentials and to identify design and implementation challenges. In this technique powder is printed layer-by-layer in the shape of the cross-sections of the part using electrophotography, which is a very widely used non-impact printing method. The electrophotography process involves picking and depositing powder using an electrostatically charged photoconducting surface. Each layer of powder is consolidated by fusing before the next layer of powder is printed. A fully automated test bed was constructed that consists of a printing system, fusing/ heating plate, a build platform that has two-degrees of freedom as well as software that drives the system. Electrophotography provides high printing resolution and accuracy that is particularly suited for printing fine powder (5-20 microns) to build small objects. In addition to rapid prototyping, applications of this process include layered manufacturing of a variety of micro and meso-scaled objects and assemblies.

15. SUBJECT TERMS

16. SECURITY CLASSIFICATION OF:			17. LIMITATION OF ABSTRACT	18. NUMBER OF PAGES	19a. NAME OF RESPONSIBLE PERSON
a. REPORT	b. ABSTRACT	c. THIS PAGE			Ashok Kumar
Unclassified	Unclassified	Unclassified	UL	39	19b. TELEPHONE NUMBER *(include area code)* (352)392-0814

OFFICE OF NAVAL RESEARCH

Electrophotographic Solid Freeform Fabrication

Ashok V. Kumar
Associate Professor
Department of Mechanical and Aerospace Engineering
University of Florida
Gainesville, FL 32611-6300
Email: akumar@ufl.edu
Phone: (352) 392-0816
Fax: 352) 392-1071

TECHNICAL REPORT

for

GRANT NUMBER: N00014-98-1-0694

October 2003

REPORT NO: ONR-ESFF-10-2003

Electrophotographic Solid Freeform Fabrication

TECHNICAL REPORT
for
GRANT NUMBER: N00014-98-1-0694

PI Name:	Ashok V. Kumar
Institution:	University of Florida
Department:	Mechanical and Aerospace Engineering
Phone Number:	(352) 392-0816
Fax Number:	(352) 392-1071
Street address:	237 MAE-B
City, State, ZIP:	Gainesville, FL 32611-6300
Email address:	akumar@ufl.edu
Home page:	http://www.mae.ufl.edu/~akumar

Grant Title:	Electrophotographic Solid Freeform Fabrication
Grant/Contract Number:	N00014-98-1-0694
Reporting Period:	June 1998 to September 2003

Table of Contents

1.1. Introduction

The objective of this research was to establish the feasibility of solid freeform fabrication by electrophotographic powder deposition. Towards this end a prototype system or test facility was designed and built that can deposit powder layer by layer, in the shape of the part cross-section, to build a part. Various powders and powder characteristics that play an important role in controlling the accuracy and precision of the system were studied. Theoretical and numerical models of image development and powder transfer process were developed to better understand the parameters that control print quality and to understand the potentials and the limitations of the process.

Figure 1 shows the schematic diagram of the Electrophotographic Solid Freeform Fabrication (ESFF) system (or testbed) [1]-[4] that was designed and built using a process patented by the principal investigator [5]. In this process, parts are built by depositing powders layer-by-layer using electrophotography [6].

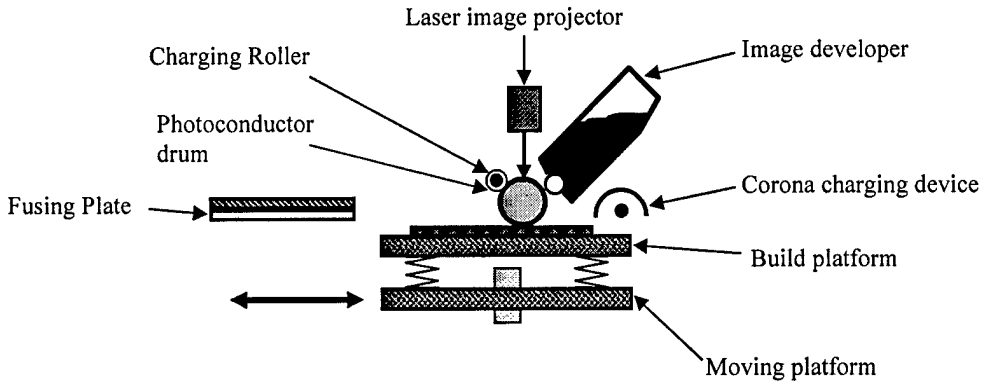

Figure 1: Schematic diagram of the ESFF system

The photoconductor drum, which is coated with photoreceptive material, is charged using a charging roller or a corona-charging device. The photoconductor drum can hold the applied charge since the photoreceptive material is an insulator in the dark. A latent image is formed on the surface of the drum by projecting laser beam on its surface to selectively discharge regions on the drum. The image developer, shown in the Fig. 1, contains the powder to be printed. The developer charges the powder and brings it to the close vicinity of the photoconductor drum so that the charged powder jumps on to the charged regions of the drum (or discharged region depending on the polarity of the powder). The image formed by the powder on the drum is then transferred on to the top layer of powder previously deposited on the build platform. To facilitate this transfer, an electric field is created between the two surfaces. The platform is moved such that there is no relative velocity between the platform and the surface of the rotating drum where it almost touches the top layer of powder on the platform. After the powder is deposited, the

platform passes under the heater (or fusing plate), which heats and compresses the top layer of powder to ensure that the powder fuses (or at least acquires sufficient green strength). This process is repeated to add the many layers of powders on the build platform. The back and forth motion of the platform needs to be controlled such that it is synchronized with the motion of the photoconductor drums.

1.2. Design and construction of a Test Bed

An Electrophotographic layered manufacturing test bed based on the concept described above was designed and built. The system was designed to be a modular and flexible experimental platform to study various ideas and configurations in which an electrophotography based layered manufacturing systems may be implemented. Figure 2 shows a photograph of the test bed with the printing system, compaction and fusing plate. A Canon electrophotography engine was used as the printing system. The build platform is mounted on linear actuators so that it can be moved in the horizontal and vertical directions. A control algorithm was implemented using C++ to drive a 2-axis commercial controller that controls the linear actuators. In addition, a program named "SolidSlicer" was implemented in Java that can read solid models from data files in STL format and "slice" them to determine the cross-sectional image that needs to be printed. The software then sends these cross-sectional images to the image projector and communicates with the C++ control software to drive the drum and platform positioning system.

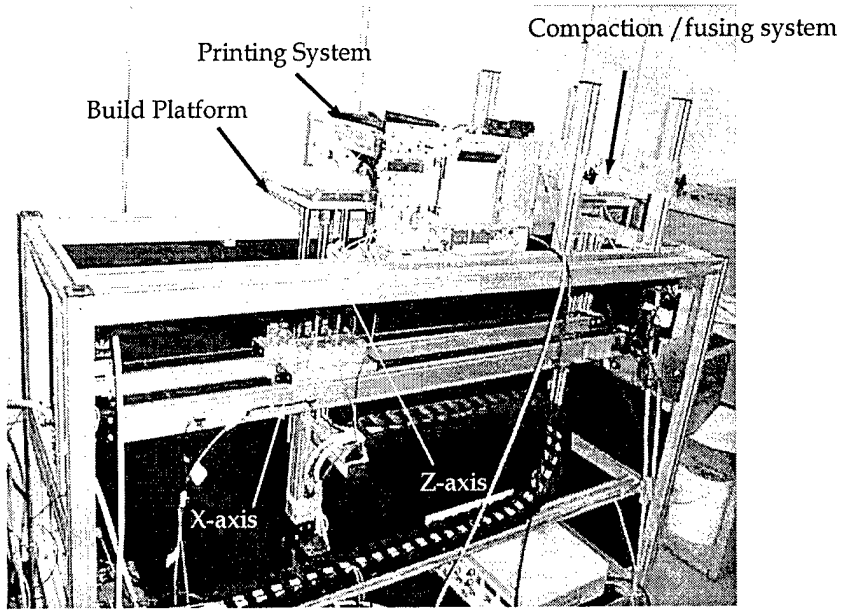

Figure 2: Photograph of the testbed

Figure 3 shows a CAD model of the test bed. A belt driven linear actuator moves the build platform in the horizontal (or x-) direction while a lead screw driven linear actuator moves the platform vertically (z-

direction). Both the actuators are driven by servo-motors controlled by a digital control system. The printing system prints powder on the build platform as it passes below the printer. The cross-sectional images to be printed are computed by software that runs on a PC and can read in the solid model of the part to be fabricated in the STL format. The powder that is printed on the build platform is compacted and fused by the compacting system which is a heated non-stick plate mounted on a rigid frame.

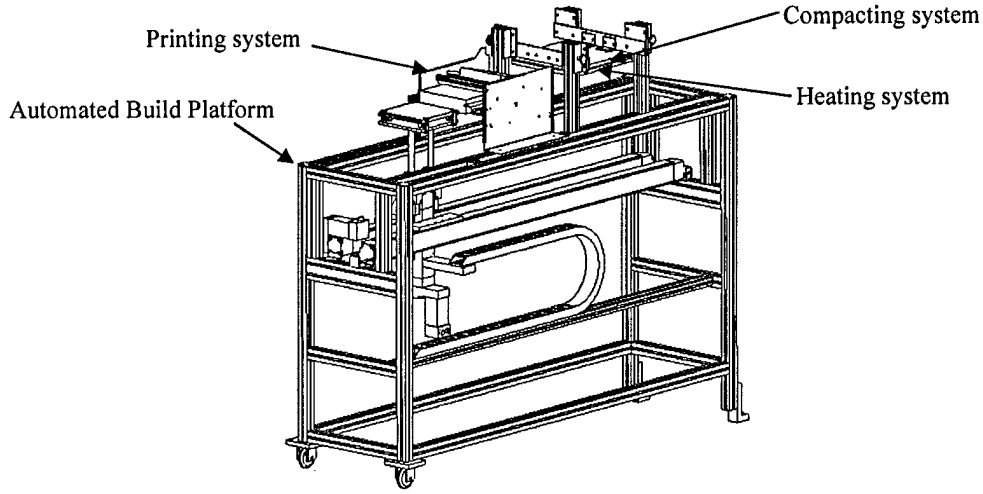

Figure 3: Model of the ESFF machine

The most important sub-system of the test bed is the electrophotographic printing system. Figure 4 shows the schematic diagram of the electrophotography engine used in a desktop laser printer from which components were taken to build the printing system for the test bed. The photoconducting drum is an aluminum drum that has a coating of photoreceptive material which is non-conductive in the dark and conductive when exposed to certain wavelength of light. When the drum rotates its surface is cleaned by the cleaner blade and then charged negative by the charging roller that is made of conducting polyurethane on which a DC biased AC voltage is applied. The uniformly charged surface of the drum is selectively discharged by the laser image scanner that projects a UV laser on the drum surface. The region on the surface of the drum that is exposed to the laser beam becomes conductive and therefore gets discharged. A latent image is thus formed on the surface of the drum consisting of the discharged areas.

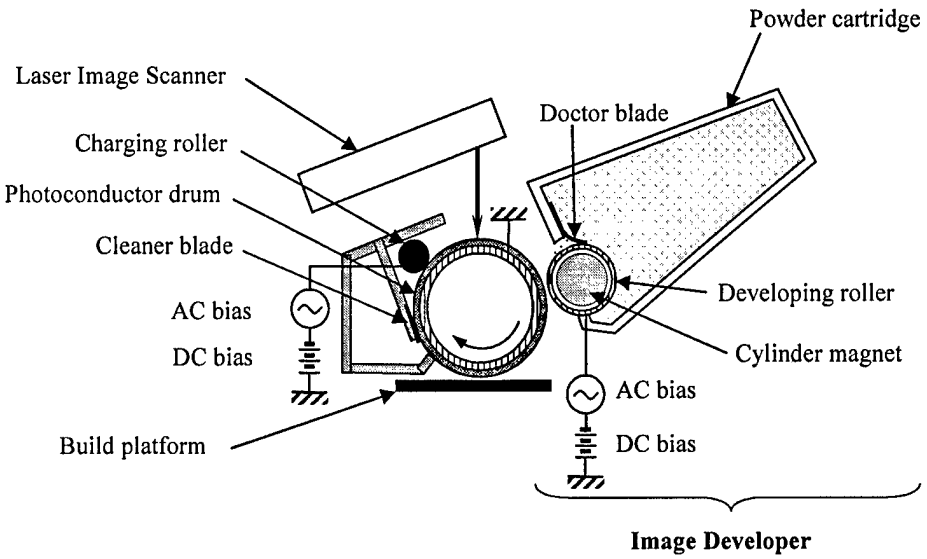

Figure 4: Schematic of the electrophotographic printing system

The latent image is converted into a real image when powder is electrostatically attracted (or developed) on to the discharged regions of the drum from the image developer. The image developer consists of the powder cartridge and the developing roller shown in Fig. 4. The developing roller is a hollow metallic roller which encases a cylinder magnet. The powder is magnetized so that it sticks to the developing roller. As this roller rotates a thin layer of powder squeezes out between the doctor blade and the roller. A DC biased AC voltage is applied to the roller to print this powder on to the photoconductor drum. The powder is electrically charged to the same polarity (negatively) as the surface of the drum so that the powder is only printed on to the discharged areas due the electric field between the developing roller and the photoconductor drum.

The image developed on to the photoconductor surface is transferred to the printing surface or the build platform of the test bed. A positive charge is applied to the surface of the platform. The field generated by this charge attracts the negatively charged powder on the surface of the drum to the surface of platform, and thus the real image on the drum surface is transferred to the platform surface. The control system synchronizes the printing with the platform motion. The platform is moved at a velocity equal to the tangential velocity of the drum so that there is no relative velocity between the two surfaces as the image is transferred from the drum to the platform.

The important subsystems of the test bed are: an electrophotography engine, flexible build platform, compaction and fusing system and controlling and monitoring software. These subsystems are described below in more detail.

1.2.1. Electrophotography engine

The electrophotography engine consists of a controller, an image formatter, a charging unit, a laser based image projection subsystem, a photoconductor drum and an image developer. The controller in the electrophotography engine controls the motors and the laser subsystem in synchronization. The image formatter translates the digital data from the PC into digital signals for the image projection subsystem. The charging unit negatively charges the surface of the photoconductor drum by direct contact charging. The image projection subsystem contains a modulated laser (700 to 750 nm wavelength) and a rotating polygonal mirror that projects the image line by line on the photoconductor drum. The laser is used to discharge the image areas (discharged area development) forming the latent image on the photoconductor drum. Figure 5 shows the photoconductor drum and an image developer designed for printing magnetic powder. The image developer consists of a powder cartridge and a developing cylinder on which a negative DC biased AC potential is applied to charge the powder and to facilitate image development.

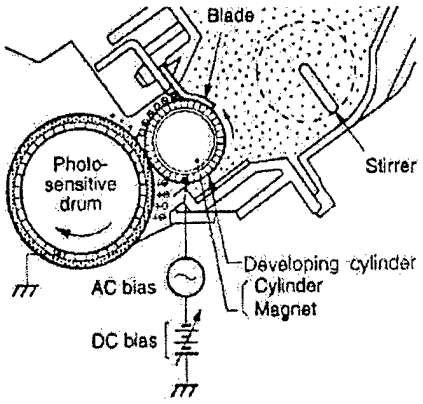

Figure 5: Image Developer

The developing cylinder is metallic and it rotates around a fixed magnetic core inside the powder cartridge. The powder is attracted to the magnetic core of the cylinder and is transported out of the cartridge as the cylinder rotates. A rubber blade meters the powder on the developing cylinder to a uniform thickness. The electric field between the development cylinder and the photoconductor drum due to the applied potential creates a powder cloud between them. Due to the negative bias voltage the powder is repelled from the developer roller on to the discharged regions of the photoconductor drum thus developing the image on it. The powder layer picked up by the photoconductor drum is then transferred on to the previously printed layers on the build platform to make the 3D part.

1.2.2. Flexible build platform

The build platform can traverse in the horizontal and vertical directions and is controlled by servo motion controller (Galil, DMC 2030). The positioning is done by servomotor actuated linear lead screw drive in vertical direction and a belt drive in horizontal direction, with rotary encoders. Homing and limit

switches are used to initialize and restrict motion to specified limits. A schematic diagram of the build platform is shown in Fig. 6.

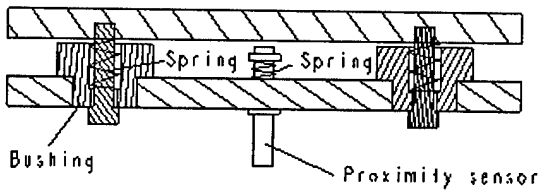

Figure 6: Flexible build platform

The top plate on which the part is built is mounted on springs so that it is flexible and does not damage the photoconductor drum or the part during the printing process. After each layer of powder is printed, the build platform is pressed against the compaction plate which is heated to a temperature at which the polymer powder will fuse. When the part is compressed the top plate of the build platform is pressed towards the bottom plate. The proximity sensor on the bottom plate is activated when the springs are compressed by the desired amount and this signal is used by the controller to determine when to stop compacting. The position of the platform after compaction is recorded and is used as a reference to set the height of the platform during printing. The proximity sensor has a static resolution of 0.3μm, which ensures accurate positioning of the part under the electrophotography engine. After each print the new reference is compared with the original position of the platform at the first print to compute the part height. The part height is used for real time slicing of the solid model. The top plate of the build platform is given a positive DC voltage, which causes the negatively charged powder image to transfer from the drum's surface to the build platform.

1.2.3. Compaction and fusing system

The compaction-cum-fusing plate consists of a strip heater sandwiched between two flat metal plates. The temperature of the plate is controlled by a temperature controller. The bottom plate of the fuser can thus be maintained at a desired temperature. Figure 7 shows the arrangement of the two plates with the strip heater. The non-stick coating on the bottom plate prevents the powder from sticking to the fuser plate.

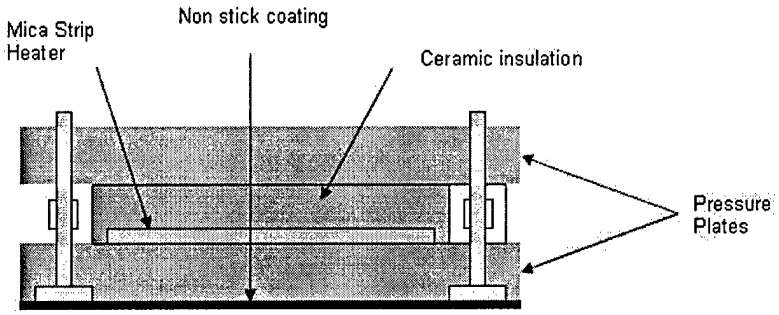

Figure 7: Compaction cum fusing platform

1.2.4. Control software for automation

The process control algorithm for the testbed consists of two components, a printing algorithm and a motion control algorithm. A software (SolidSlicer) was developed, to implement the overall algorithm. It has a graphical user interface implemented in Java and Java3D that enables the user to read in 3-D CAD data file (STL format) to display it as well as to interactively position it relative to a coordinate system on the build platform. The software can also slice the solid model to determine the cross-sectional image at any z-level (height from the platform) and send this image to the printing system. After positioning the solid model as desired, when the user interactively initiates the printing process, the motion control algorithm and printing algorithms run simultaneously. The motion control algorithm is implemented partly in C++ and partly in the command language of the motion controller. The algorithm is illustrated using a flow chart in Fig. 8.

The motion control algorithm and the printing algorithm are run as two separate threads that communicate with each other so that they can run simultaneously. At the beginning of the process, the motion control algorithm initializes all subsystems, turns on the fusing heater and moves the build platform to the home position along the x and the z directions. Thereafter, the platform is moved under the compaction plate to set the z-level. The build platform is supported on springs that are mounted on the z-axis bottom plate, as explained earlier and shown in Fig. 6. It is moved up against the compaction plate until the springs compress by a desired amount which is detected by a proximity sensor. This ensures that the compaction pressure is the same during every compaction. The level at which the platform stops is used as a base line from which the new z-level of the platform for printing is set. This ensures that as the part height grows, the z-level of the platform is lowered after each compaction. After setting the z-level, the status of the testbed platform is set as "ready". This signal and the current z-level are communicated to the printing algorithm and the platform is moved to a start position where it waits for a signal from the electrophotography engine that the printing has started.

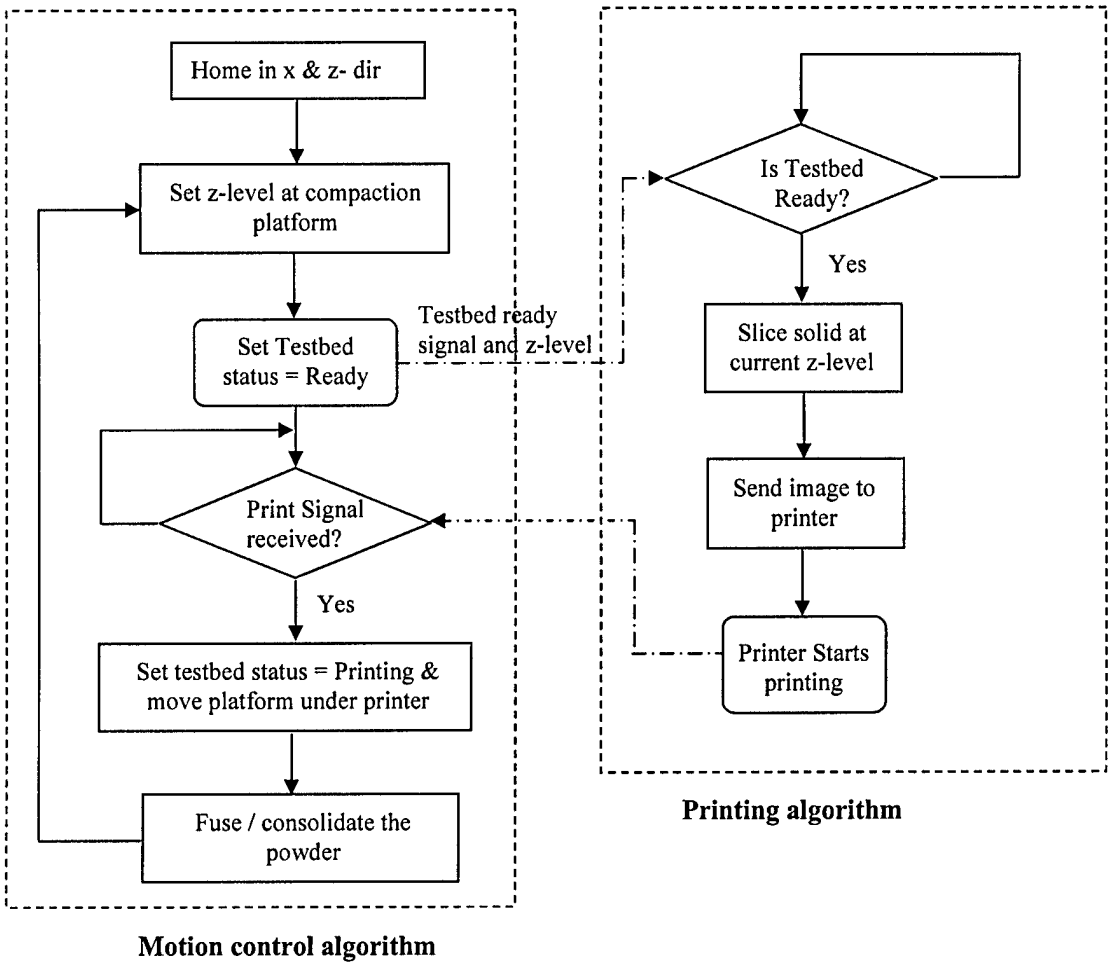

Figure 8: Process control algorithm

When the printing algorithm receives the signal that the test bed is ready, it slices (or computes the cross-section of) the solid model at the current z-level and creates 2D cross-sectional image. This image is then sent to the electrophotography printing engine for printing. When printing begins a signal is sent back to the motion control algorithm, which begins moving the platform under the printer at speed equal to the linear speed of the surface of the photoconductor drum. This ensures that the motion of the platform is synchronized with the rotation of the photoconducting drum and that images printed on each layer are properly aligned. After the printing is completed the platform travels under the compaction and fusing plate that heats the powder to fusing temperature (180°C-200°C for the polymer powder used in our experiments). By comparing the new z-level with the previous z-level, the layer thickness can be computed. The motion control algorithm once again sets the status of the testbed to ready and sends the signal to the printing algorithm along with the new z-level. The motion controller then once again positions the build

platform at the start position and waits for the signal from the printing system. This process is repeated until the 3-D solid model is constructed. The compaction pressure, the fusing time and the temperature of the heater are all important process parameters which determine the quality of the part.

1.3. Theoretical models of powder transfer

The research conducted thus far has shown the feasibility of printing powder layer by layer using the electrophotography method. The testbed that was built using this technique can print polymer powders layer by layer with precise alignment between layers. The system is now fully automated using control software that runs on a PC. After each layer of powder is printed the powder is fused by radiant heater or mica strip heaters.

The material used is toner powder consisting of styrene with various additives including ferrous oxide to magnetize the powder. The particles in the powder were approximately 5 microns in size. A constant DC voltage of 1000V was applied to the aluminum build platform to enable printing. The layer thickness is dependent on particle size as well as parameters such as charge per unit mass of powder, speed ratio between photoconductor drum and developer roller etc. It was found that the powder transfer per print decreased with increasing part height. The amount of powder transferred from the electrophotography engine to the build platform decreased with part height and stopped after a certain part height. This problem is illustrated in the Figure 9.

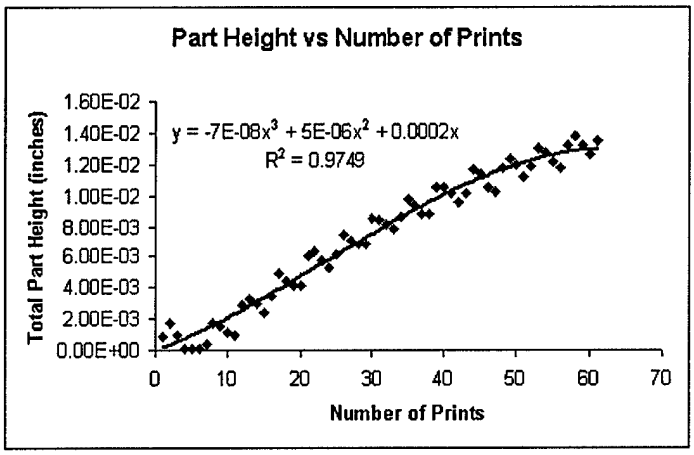

Figure 9: Plot of the part height with the number of prints

The software computes the part height based on the readings taken by the proximity sensor during the build process. Figure 9 shows the plot of part height versus the number of prints. The electrostatic analysis of the powder transfer from the photoconductor drum to the build platform revealed the cause of this

problem. Figure 10 shows the schematic diagram of the transfer zone where the photoconductor drum and the build platform are modeled as parallel plates.

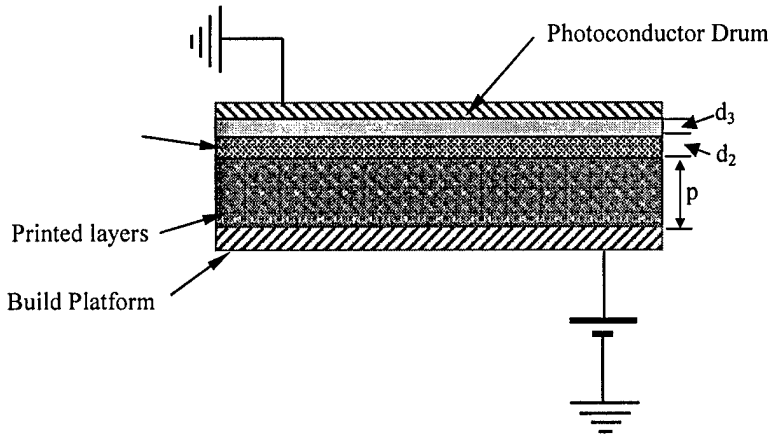

Figure 10: The parallel plate analogy of the transfer zone

Applying Gauss's law [7], the electric field at the interface between the previously printed layers and the fresh powder layer on the photoconductor drum can be determined as shown in Eq. (1). This electric field causes the fresh toner to transfer from the photoconductor surface on to the top of previously printed layers.

$$E(p,V_{DC}) = \frac{V_{DC} + \rho_1 \frac{p^2}{2K_1\varepsilon_0} + \rho_2 \frac{d_2^2}{2K_2\varepsilon_0} - \rho_3 \frac{d_3^2}{2K_3\varepsilon_0} + \rho_2 \frac{d_2 p}{2K_1\varepsilon_0}}{K_2\left(\frac{p}{K_1} + \frac{d_2}{K_2} + \frac{d_3}{K_3}\right)} \quad (1)$$

In the above equation, V_{DC} is the potential applied to the build platform, p is the height of the part (or previously printed layers), $d_2 = 20\text{x}10^{-6}$ m (thickness of the fresh powder layer), $d_3 = 1\text{x}10^{-6}$ m (thickness of the photo-conducting layer), $K_1 = 3.42$ (permittivity of the fused powder layer), $K_2 = 3.42$ (permittivity of the fresh powder layer), $K_3 = 3$ (permittivity of the photoconductor material), $\rho_1 = 0$ coulomb/m^3 (charge per unit volume in the fused powder layer), $\rho_2 = -1 \times 10^{-4}$ coulomb/m^3 (charge per unit volume in the fresh powder layer), $\rho_3 = 0$ coulomb/m^3 (charge per unit volume in the photoconductor layer) and $\varepsilon_0 = 8.85\times10^{-12}$ coulomb/mV (permittivity of the air).

In Fig. 11, the electric field, E, at the interface of fresh powder layer and the top layer of part is plotted as a function of the height of the part p using $(V_{DC} = 1000\text{V})$. From this figure, it is clear that the electric field decreases drastically with the increase in the height of the part (or the thickness of the previously printed and fused powder layers). This explains why the printing rate decreases with part height.

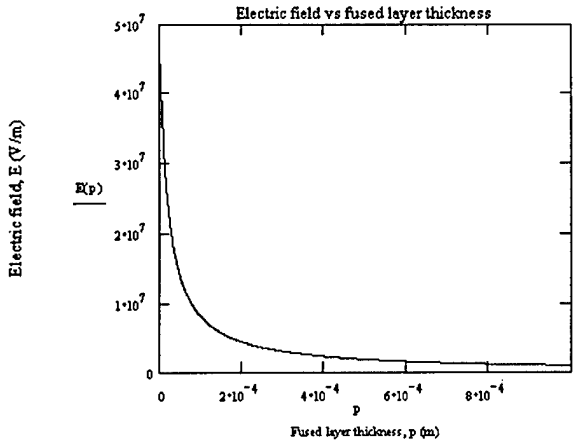

Figure 11: The plot of electric field strength at the interface of fresh powder layer and print surface

To make parts taller than a millimeter it necessary to charge the printing surface which is the top of the platform or the previously printed layer. If the top surface of the fused toner layer is charged with surface charge density, σ_s opposite to that of the fresh powder then the electric field at the powder transfer interface is as shown in equation (2).

$$E(p,\sigma_s)=\frac{V_{DC}+\rho_1\frac{p^2}{2K_1\varepsilon_0}+\rho_2\frac{d_2^2}{2K_2\varepsilon_0}-\rho_3\frac{d_3^2}{2K_3\varepsilon_0}+\frac{p}{K_1\varepsilon_0}(\sigma_s+\rho_2 d_2)}{K_2\left(\frac{p}{K_1}+\frac{d_2}{K_2}+\frac{d_3}{K_3}\right)} \tag{2}$$

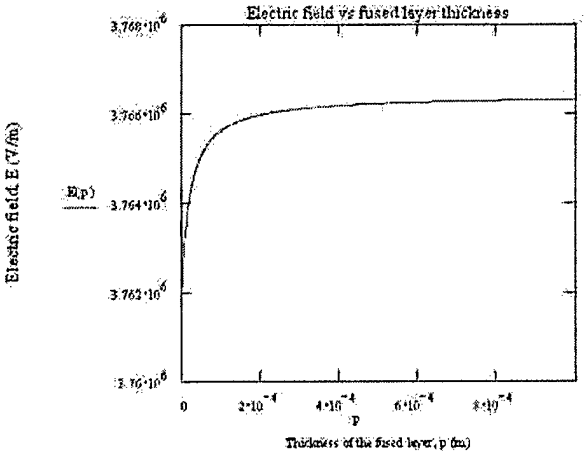

Figure 12: The plot of electric field strength at the interface of the fresh powder layer and the photoconductor

Figure 12 shows a plot of electric field, E, versus part height, p, when the top surface of the part is assumed to have a charge density of $\sigma_s = 10^{-4}$ coulomb/m^2 and the potential applied to the platform V_{DC} = 79 V. It is evident that charging the top surface helps and the electric field strength remains more or less steady and does not change significantly with part height.

A surface can be electrically charged by either contact charging using a charging roller or by corona charging. Both the methods were tried but there is a limitation on the amount of charge that can be transferred to the receiver by charging roller. The corona charging device was found to be effective for this application. The device is schematically shown in Fig. 13.

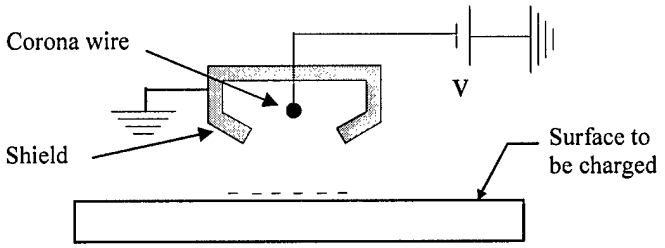

Figure 13: Corona charging device

The corona charging device consists of a corona wire encased in a metal shield that is open on one side. High voltage is applied to the corona wire and the shield. Due to this high voltage, the air near the wire is ionized creating a corona around the wire. Since the ions have the same polarity as the wire and the shield, they are repelled from the wire towards the surface being charged.

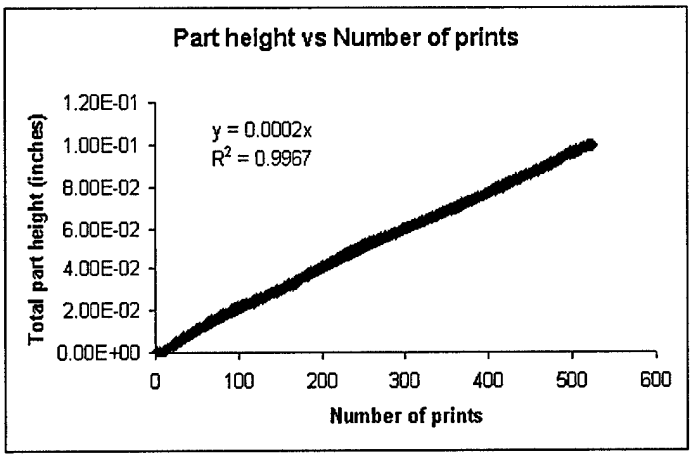

Figure 14: Plot of the part height with the number of prints with the corona charger

Figure 14 shows the plot of part height versus number of prints when a corona charging device is used to charge the top layer of the part before every layer is printed. Figure 15 shows the parts built by test bed

with the corona charger. The parts are approximately 3 mm tall and took about 575 layers of polystyrene based toner powder. The build platform is approximately 8x8 in and all the parts shown in Fig. 15 were built simultaneously. The slope of the curve in Fig. 14 indicates a constant material deposition rate of about 5 microns per print over the total building time. This low rate of printing can be improved by more efficient removal of residual charge from the previously printed layers and by increasing the charge density deposited by the corona charging device.

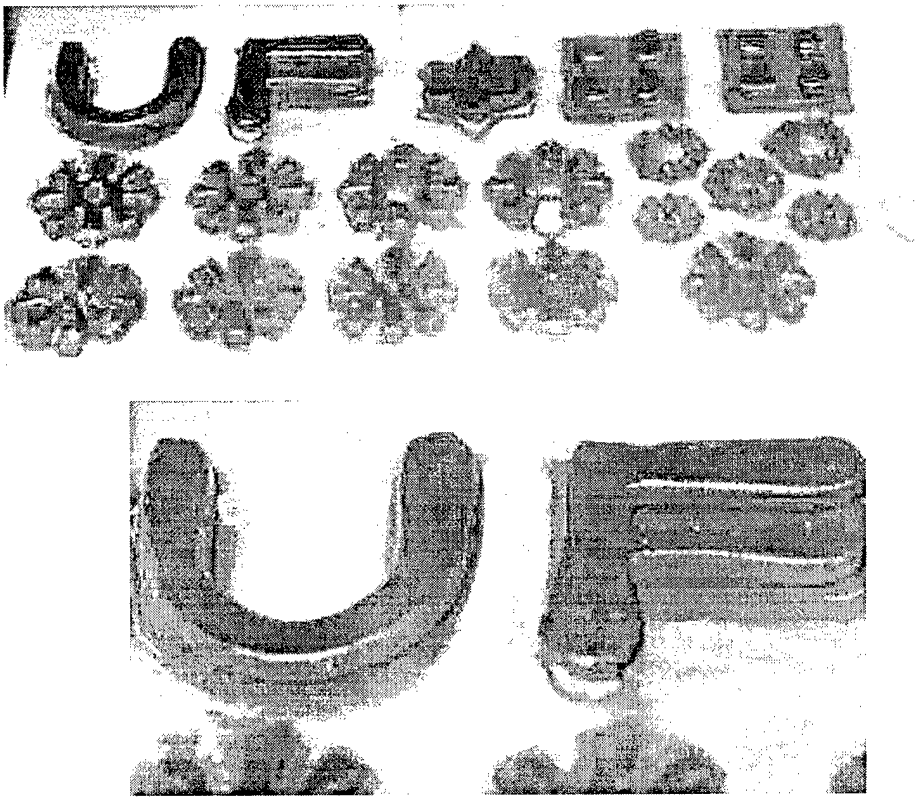

Figure 15: Parts made by the test bed with corona charger

Electrophotographic printing technology is capable of achieving very high resolution of up to 2400 dpi (dots per inch). In the test bed described in this paper, the printing system is capable of achieving up to 600 dpi. However, the accuracy of the parts made using the process also depends up on the accuracy with which subsequent layers can be aligned over each other. Another factor that affects the part accuracy is the distortion occurring during the fusing and compaction after each layer is printed. Further research is needed to understand the role of all these factors that must be carefully controlled to achieve desired tolerance and surface finish for the parts.

1.4. Modeling of electric field due to latent image

The field created by the latent image (or charged region) on the drum is important to study because non-uniformity of this field leads to non-uniformity in the print. The field is stronger near the edges of image due to which more powder is developed near the edges than at the center of the image.

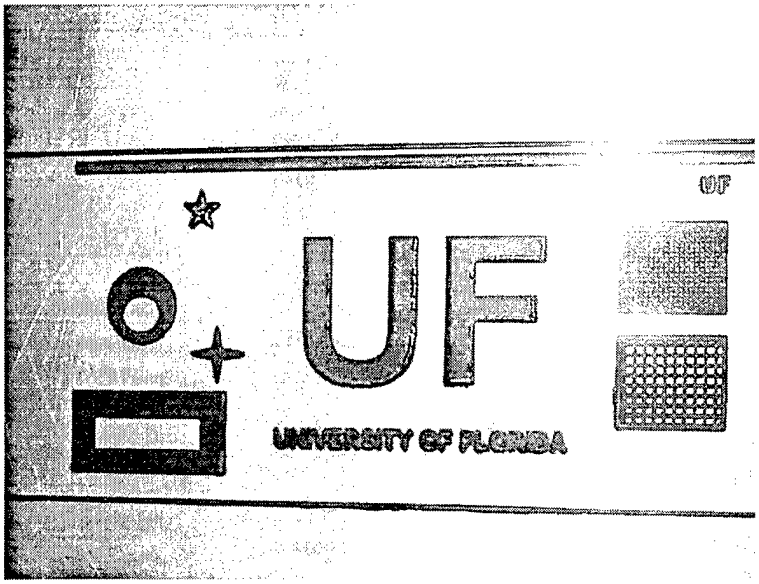

Figure 16: Parts built on an aluminum build-platform

Figure 16 illustrates fifty layers of toner powder printed directly on an aluminum platform. The same image was printed repeatedly to create parts approximately 1 mm high. The images were fused by a radiant heater and not compacted after each print. It is clear that the edges of the image grow faster due to which the edges are thicker than the interior of the image. This effect is due to the fact that the electric field at the edge of the image is of much higher magnitude than that in the center. This effect is not seen in the printing of thin lines because the entire print area is within the range of the strong field. To study this further we developed a finite element model to predict the electric field generated by the latent image. The physical model of the system is shown in Fig. 17 with the simulation results shown in Fig. 18. The left half of the figure is the image area where there no charge on the surface so that powder can print on to this region. Although the field in the middle of the image here appears to be zero, it is in fact roughly 3.6×10^7 N/C, several orders of magnitude smaller than the value at the edge but still positive. This large difference in electric field enhances printing along the edges of a solid image. When a radiant heater is used to fuse the powder (without compaction) the edges grow faster. However, when a heated compaction plate is used for fusing the powder, it flattens the top layer during compaction after each print. Even though this eliminates the edge enhancement, the excess powder that was printed along the edge gets pushed sideways causing

distortion of the edge and affecting the accuracy. This problem may be alleviated if support powder is printed that surrounds the part powder before compaction.

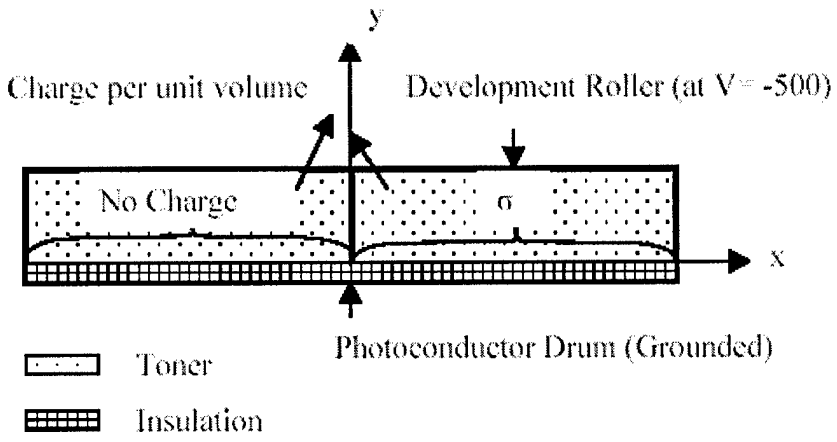

Figure 17: Model of solid area printing

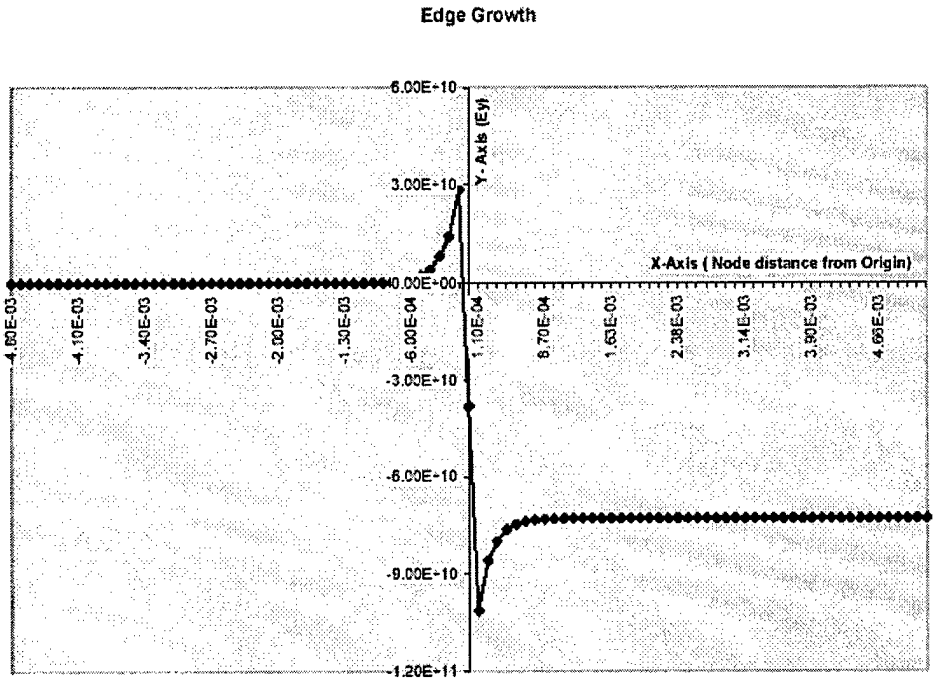

Figure 18: Solid area printing model results

Due to the stronger field strength at the edges of the solid area more powder is printed along the edge. In the same way more powder gets printed along lines since electrostatic images of thin lines create strong electric field. Therefore, it was felt that if a pattern of lines (like hatching lines) are printed within the cross-sectional image rather than printing solid area it would give better prints that do not have edge enhancement. To study this, a FEA model of an alternating line pattern with lines of width 0.2 mm was developed. A unit of the repeating pattern was modeled with several elements along the length of both the charged and discharged areas. The model in this simulation is shown in Fig. 19, with the simulation results in Fig. 20. The charged area is in the center, with the discharged image areas on either side.

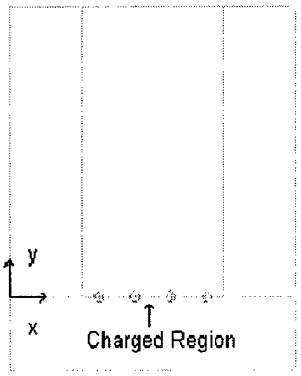

Figure 19: Pattern printing model

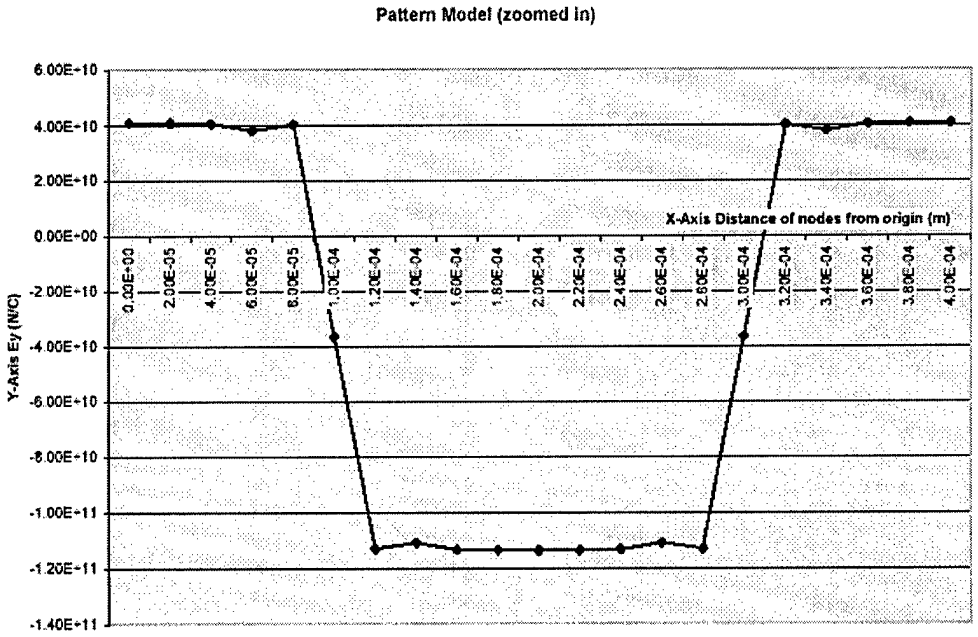

Figure 20: Pattern printing model results

This simulation shows that a much stronger field is created by this pattern within the charged area as well as in the discharged area with the edge effect is much less noticeable. There is a near-uniform field across the image area, meaning a more consistent transfer of toner in regards to image field. Thus pattern printing offers the possibility of eliminating the edge effect and enhances printing along the lines of the pattern. However, no powder will be printed between the lines so the overall mass per unit area printed may be less. The next step would be optimizing the pattern print in terms of both hardware and software for the actual system and testing how it worked when applied. This work is currently in progress.

1.5. Printing binder on powder bed using electrophotography

An alternative way to build parts using electrophotography is to print a binder powder on uniformly deposited part powder as is done for 3D printing. The binder powder can then be fused thermally so that it diffuses into the part powder and binds the part powder on subsequent cooling and solidification. The success of this concept depends on the ability to deposit thin uniform layers of part powder and the efficiency with which the binder powder can be printed on to the part powder bed. It is not feasible to transfer powder directly from the photoconducting drum on to previously deposited part powder bed because the charged regions of the drum will pick up some part powder. In other words, during the transfer process, some part powder will get picked up by the photoconductor drum especially on its charged areas. This can quickly damage the photoconductor especially if the part powder is abrasive. To protect the photoconductor drum and to minimize part powder reverse printing it is necessary to use either a transfer roller or a transfer belt. The ideas is that the binder can be first printed on to an intermediate transfer device and then subsequently transferred from this device to the part powder bed. Figure 21 shows the concept schematically where a transfer roller is shown between the photoconductor and the build platform. Shown on the right is an equivalent parallel plate model for the interface between the photoconductor drum and the transfer roller as well as the interface between the transfer roller and the print surface.

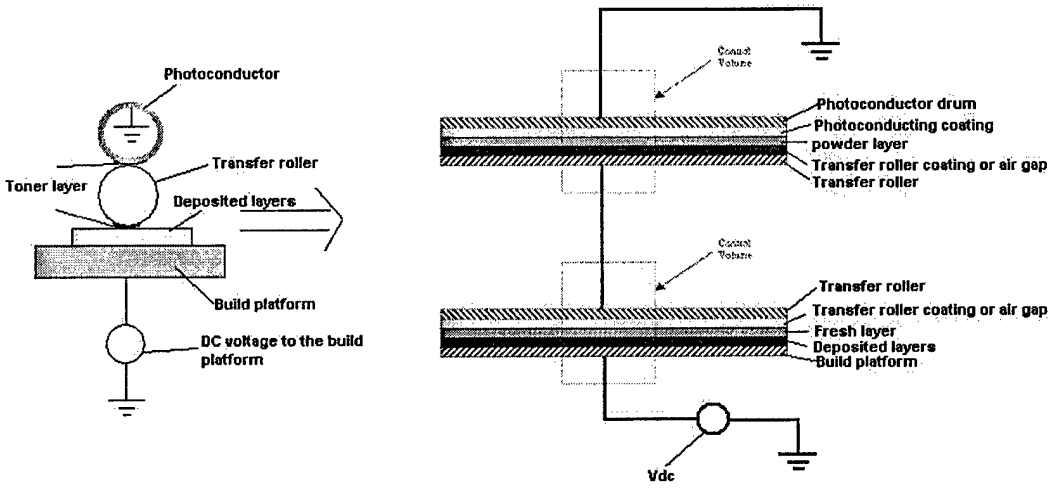

Figure 21: Parallel plate analogy for transfer device arrangement

Electric field is required at both interfaces to enable transfer of powder. A conductive (aluminum) drum was used as the transfer roller. The electric field for transfer can be created by applying a voltage to the build platform or by charging the top layer of the powder bed. Since the transfer roller is conductive its voltage is constant and the electric field created at one interface is transmitted to the other interface. The transfer roller rotates such that it has the same tangential velocity as the photoconductor drum so that the image can transfer from the photoconductor to the transfer roller. Similarly the build platform moves at the same velocity as the tangential velocity of the transfer roller to enable undistorted transfer of the image from the transfer roller to the platform.

If the part powder is metallic (conductive), it tends to get charged by the electric field and jumps back and forth between the transfer roller and the powder bed creating a powder cloud as shown in Fig. 22. The reason for this powder oscillation is that the conductive powder particles loose their charge and get reversely charged due to the field as soon as they contact the transfer roller or the powder bed both of which are conductive. This oscillation causes many problems including poor transfer of binder powder as well as distortion of the image. If the drum is covered with a thin insulator layer then the particles cannot loose charge to this layer and sticks to it resulting in reverse printing. Therefore this approach appears to be infeasible for conductive part powders unless some other means is used to hold down the part powder, such magnetic force if the part powder is magnetic.

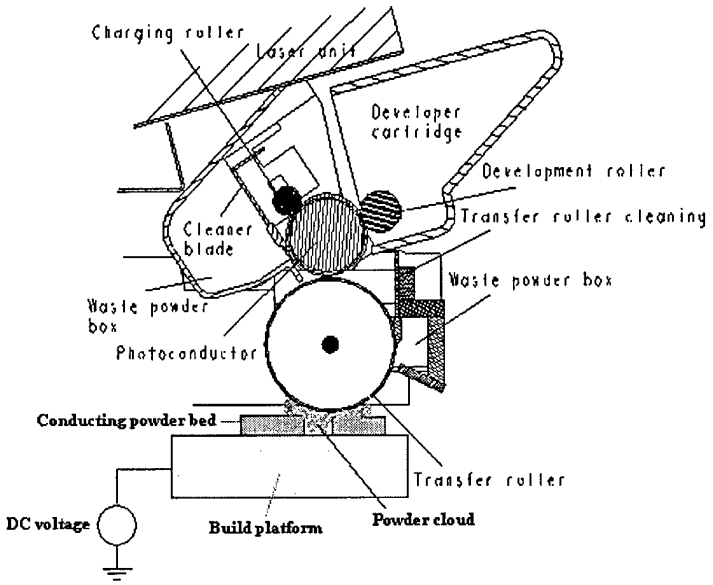

Figure 22: Transfer roller system with conducting part powder bed

For non-conductive part powders, the top surface of the powder bed must be charged to facilitate (or create the necessary field for) transfer of the binder powder. The charged particles on the surface need to be held down so that they do not get picked up by the transfer roller. Figure 23 shows a polystyrene binder powder printed on a ceramic (alumina) powder bed. The powder bed was created by spreading a layer of the ceramic powder uniformly and then it was compacted to impart green strength in order to minimize reverse printing. A thin polymer (insulator) cover was glued over the transfer roller to minimize chances of sparking between the photoconductor drum and the roller.

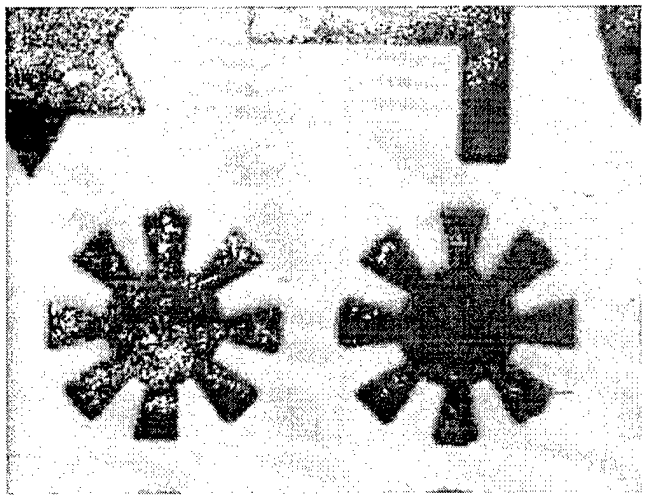

Figure 23: Toner powder on insulating alumina powder bed

In Fig. 6, the black binder powder is printed on alumina (white) powder bed. The white spots within the printed image were caused by reverse printing where the alumina powder was picked up by the transfer roller instead of the binder getting printed on the alumina powder bed. Another problem with this approach is that if the binder is too viscous after melting it may not diffuse into the part powder deep enough to ensure proper bonding between layers.

The transfer roller can not prevent reverse printing but it protects the photoconductor drum from damage. Printing binder powder for 3D printing has other disadvantages that traditional 3D printing does not have including the need for melting the binder and poor bonding between layers.

1.6. Experimental study of powder characteristics

The material characteristics of the powder used in the developer plays an important role in the electrophotography process. The three important powder properties, which determine the behavior of the powder during the electrophotography process, are the volume resistivity, permittivity and the mass density. The powder charging method that is most suitable for a given powder depends on the volume resistivity of the powder [6]. The powder permittivity determines the electric field in the development zone responsible for the development. The mass density of the powder and the density of the powder material are required to compute the packing fraction of the powder. The mathematical models developed for image development and transfer requires values for these powder characteristics.

The material that was experimentally investigated is the toner powder which is a styrene powder with additives including carbon black and charge control agents. The particles in this powder are spherical and the average size of the toner particles is $10\mu m$. A resistivity test cell was designed to test the volume resistivity of the powder and a capacitance test cell was designed to measure the permittivity. The mass density was calculated by measuring the volume and mass of the powder.

1.6.1. Powder Volume Resistivity Test Cell

The schematic diagram of the resistivity test cell is shown in Fig. 24. Volume resistivity is a property of the material regardless of its dimensions. Volume resistivity, ρ, can be defined as resistance, R, of a unit length of the material per unit area of cross-section. The resistivity of powder in the test cell can be computed as,

$$\rho = \frac{RA_{eff}}{d} \text{ where, } R = \frac{V}{I} = \text{Resistance} \tag{4.2}$$

A voltage, V, is the applied across the electrodes of the test cell and the current I is measured using an electrometer. A_{eff} is the effective area of cross-section of the powder through which the current flows and d is the gap between the electrodes.

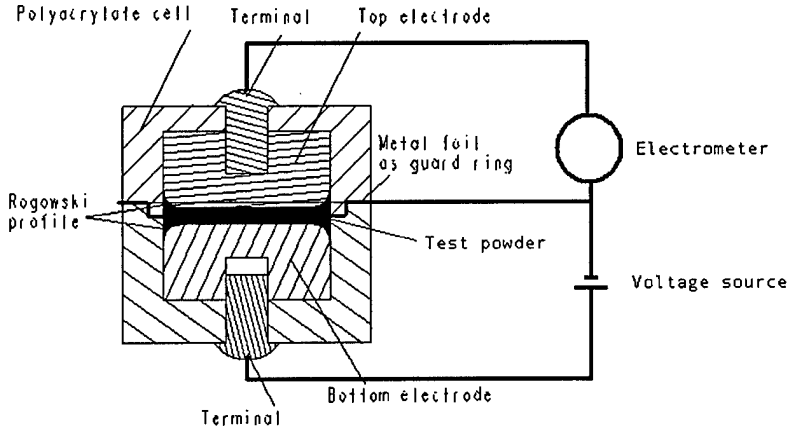

Figure 24: Parallel plate powder resistivity test cell

The electrodes should to ideally have cross-sectional profile called Rogowski profile [7] to ensure uniform electric field within the test cell. If flat face electrodes are used then the resulting parallel plate capacitor will have regions of higher field strength along the circumference of the electrodes due to fringe effects. The volume resistivity measurement requires a uniform field in between the electrodes. If flat electrodes are used, the area of cross-section that is used to calculate resistivity must corrected to account for the non-uniformity of the field. The effective area of the electrodes can be computed by the following equation [7],

$$A_{eff} = \pi\left(\frac{D}{2} + B\frac{g}{2}\right)^2 \tag{4.1}$$

In the above equation, D is the outside diameter of the circular electrode, g is the gap between the guarded electrode and the ring electrode, B is the effective area coefficient which is found by comparing the readings from the designed test cell and the one that is already calibrated. B is typically near to zero [8] for electrodes with relatively small gap, d, between the electrodes. It is thus approximated as zero. These parameters are illustrated in Fig. 25.

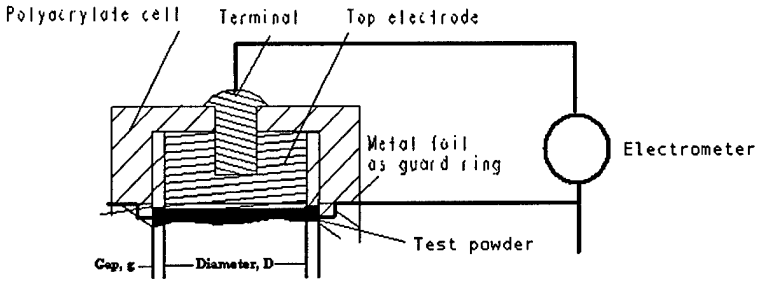

Figure 25: The volume resistivity test cell

The guard ring is grounded or given same potential as that of the low voltage electrode. The guard ring prevents the flow of current between the electrodes via the surface. No current flows between the low voltage electrode and the guard ring because they are at the same potential. The current flow from the high voltage electrode to the guard ring is not passed through the electrometer. The cell is made of polyacrylate, which is a very good insulator.

The Keithley 6517A Electrometer was used as a Pico-ammeter in this case. The specifications of the electrometer are tabulated in Table I.

Table I: Measurement ranges of the 6517A Keithley electrometer

Current Range	Voltage Range	Charge Range	Resistance Range
100 aA to 20 mA	10 μV to 200 V with 200 TΩ input impedance	10 fC to 2μC	1Ω to 10^{17} Ω with 200 TΩ input impedance

For high resistance materials the current is very low so the background currents cause large errors [8]. Alternating polarity resistance test implemented in the Keithley electrometer is used to measure the resistance and hence the resistivity. In this test the voltage is alternated between two values and the current reading is taken at the end of each time interval. The resultant current is the computed as a weighed average of the latest four measurements each at the end of a separate alteration. The first few readings are discarded so that the material assumes a steady state in that time. The experimental readings are listed in Table II.

Table II: Experimental readings from volume resistivity test cell with toner powder

RUN #	Area, A_{eff} (m^2)	Thickness, d (m)	R (ohm)	$\rho = \frac{RA_{eff}}{d}$ (Ωm)
1	5.07×10^{-4}	1.91×10^{-3}	1.7204×10^{14}	4.57374×10^{13}
2	5.07×10^{-4}	1.91×10^{-3}	2.0661×10^{14}	5.33464×10^{13}
3	5.07×10^{-4}	1.91×10^{-3}	1.7803×10^{14}	4.73299×10^{13}
			Mean	4.88046×10^{13}

In the experiments, the tests were done with a 15 seconds interval between voltage alternations and discarding the first three readings. The powder was packed in the test cell without any addition pressure other than the weight of the powder. The voltage was altered between $\pm 50V$ and three sets of test runs were done. The volume resistivity has been computed as the average value of the three tests and was found to be $4.88046 \times 10^{13} \Omega m$.

1.6.2. Permittivity measurement

The schematic of the capacitance test cell for measuring permittivity of powder is shown in Fig. 26. The powder is packed in between the disc like electrodes in a polyacrylate cylinder. The packing fraction of the powder is that for packing under gravity. The diameter, D, of the circular electrode is much larger than the gap, d between the electrodes and thus the fringe effects can be neglected. The capacitance of this parallel plate configuration is,

$$C = \frac{\varepsilon_r \varepsilon_0 \pi D^2}{4d} \tag{4.3}$$

Therefore, if the capacitance of the cell can be determined then the relative permittivity, ε_r, of the powder between the electrodes can be computed.

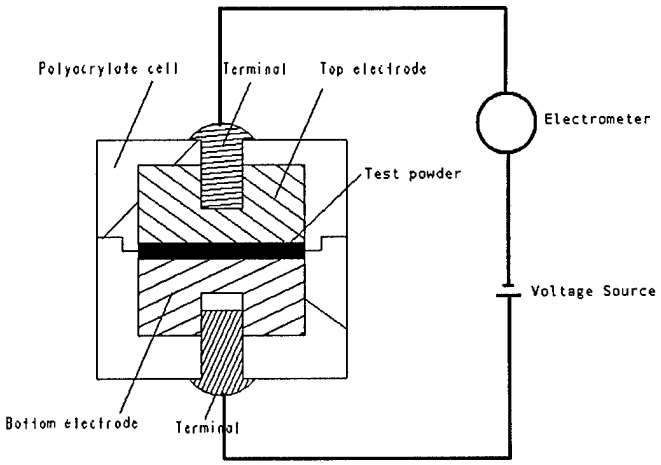

Figure 26: Parallel plate powder capacitance test cell

The powder has a finite resistivity therefore some current flows through it therefore the system can be modeled as a capacitance and a resistance in parallel as shown in Fig. 27. The current flow through the circuit, I, measured by the electrometer therefore is the sum of the current charging the capacitor, I_c, and the leakage current through the resistance, I_R.

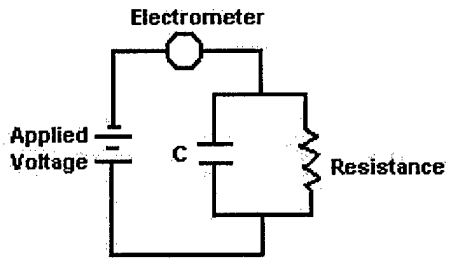

Figure 27: RC analogy for capacitance test cell

The current, I_C, charging the capacitor decreases exponentially with time whereas I_R remains constant. After substantial time, about five times the time period of the circuit, I_C would be negligible as compared to I_R. Subsequently, when the capacitor is disconnected from the voltage source, the charge in the capacitor gets discharged through the resistance, R. The Keithley electrometer has "capacitor leakage current test" functionality to measure leakage current in wires. This function, with minor modification in the setup, was used to calculate the decaying current in the capacitance test cell. A voltage applied across the capacitor, to charge the capacitor. When the capacitor is fully charged a steady state is reached and the current in the circuit is constant. The applied voltage when divided by this steady state current gives the resistance, R. During charging, the decaying current depends on the voltage applied and the permittivity of the powder. The time constant of this plot is equal to RC where the resistance R is already measured. The capacitance, C can be found since the resistance, R, and the time constant, T, are known. The capacitance, C=Q/V can also be found if the corresponding area under the curve is calculated, which will give the charge, Q on the capacitor and the applied voltage, V is known. One such plot is shown in Fig. 28. Table III lists the readings from experiments where the permittivity was measured using the capacitance test cell.

Table III: Experimental readings from capacitance test cell

RUN	T (sec)	R (GΩ)	C=T/R (Farad)	$A=\frac{\pi D^2}{4}\ m^2$	g (m)	$\varepsilon_r=\frac{C4g}{\varepsilon_0\pi D^2}$
1	0.470	56.2	8.36299E-12	0.000506451	0.001905	3.554480
2	0.440	55.3	7.95660E-12	0.000506451	0.001905	3.381755
3	0.448	55.6	8.05755E-12	0.000506451	0.001905	3.424663
4	0.442	54.8	8.07007E-12	0.000506451	0.001905	3.429983
5	0.399	51.4	7.77121E-12	0.000506451	0.001905	3.302958
						3.418768

T = time constant
R=resistance
C=capacitance
A=area of the plates
g=gap between the plates
ε_r = relative permittivity

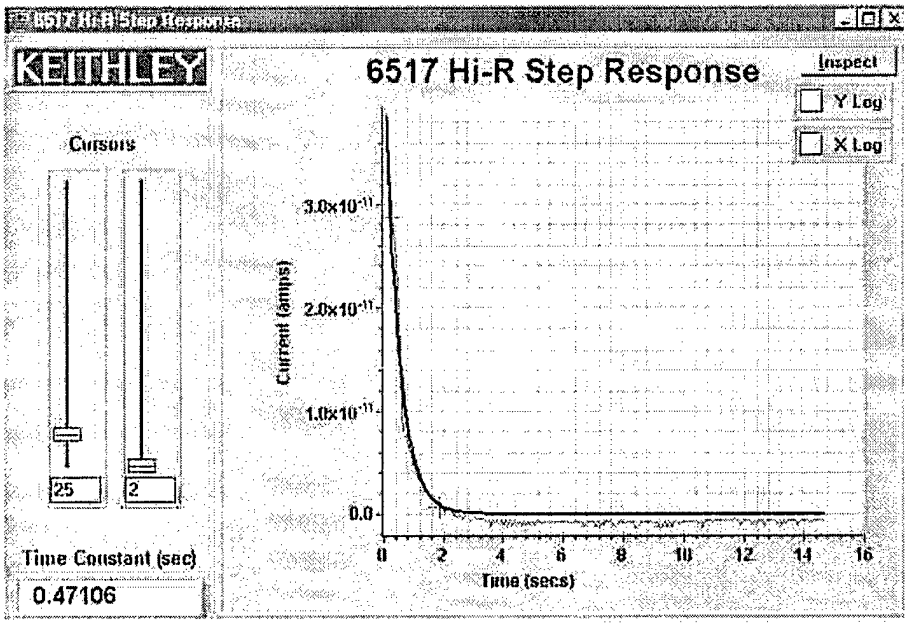

Figure 28: The current verses time plot for capacitance measurement

As the table shows, the average relative permittivity for the toner packed by its own weight was found to be 3.42 .

1.6.3. Measuring the Mass Density

The mass density of the powders was calculated for powder packed under gravity (its own weight). The powder was allowed to settle in a measuring cup under gravity and the mass of the powder with the cup was measured in the Scientech electronic weighing balance. Since the mass of the cup is known, the mass of the powder can be determined, which divided by the volume of the measuring cup gives the mass density. Table 4-5 lists the specifications of the SA 410 series Scientech balance.

Table IV: Specifications of the SA 410 Scientech balance

Capacity	Readability	Weighing speed	Repeatability (standard deviation)	Linearity
410 gm	0.0001 gm	Adaptive	0.00015 gm	±0.0002 gm

Table 4-6 lists the measurements for the two powders used on the ESFF test bed.

Table V: List of mass density of toner powder

Mass with the cup (gm)	Mass of the powder (gm)	Volume of the cup (cm^3)	Mass density (gm/cm^3)
10.6864	9.4982	10	0.94982

Powder characteristics determined experimentally provided insight into the electrophotography process. Resistivity of $4.88046\times10^{13}\Omega m$ implies that the toner powder is a good insulator. According to Schein [6], the charging mechanism suitable for powder with such high resistivity is injection charging or triboelectric charging. The relative permittivity of the toner and its mass density that was found experimentally were used in the theoretical analysis of the development process, as described earlier, to determine the development parameters in the development zone.

1.7. Design of Image Developers

The developer system in a printer is the system responsible for developing powder on to the photoconductor surface thus turning the latent (or electrostatic) image into a real image. A typical development system stores the powder, charges the powder, transports the powder, and transfers the powder to the photoconductor surface.

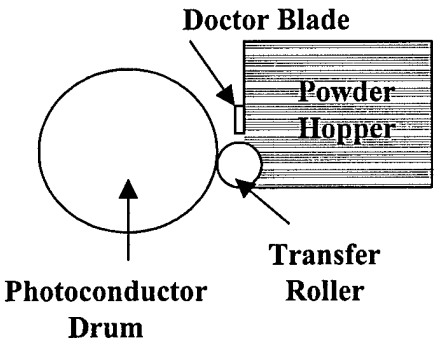

Figure 29: Development system schematic

A simplified schematic of a development system is shown in Fig. 29 where the main components of the system are labeled. The powder hopper is a receptacle filled with powder. The doctor blade is a metering device used to control the thickness of the powder layer being brought out of the hopper, and is often a part of the charging system. The transfer roller serves to move the powder and bring it near the photoconductor drum.

1.7.1. Developer system fundamentals

a) Powder Storage

The storage of powder is a very straightforward part of the development process. In general, developers will have a hopper of some variety filled with toner powder. Some contain a stirring apparatus to prevent the very fine toner powder from agglomerating into a solid mass. Many commercial systems will also have

specially designed access points to allow for refilling of the cartridge during recycling, and some new developers contain electronic safeguards to prevent unauthorized recyclers from tampering with the cartridge. The main concerns in this stage are that powder be prevented from leaking, and that it be possible to replenish the powder supply when necessary.

b) Powder Charging

The proper charging of powder is critical to the electrophotographic imaging process. If powder is not adequately charged, it will not transfer to the image areas. If it is too highly charged, a very thin layer of powder on the image will be sufficient for charge cancellation and the image will be very faint. If the powder is not charged consistently there will be noticeable variations in imaging between prints or even within an image. If powder charges to the wrong sign, there will be background printing in the final result. There are currently three main methods used for powder charging: corona charging, injection charging, and triboelectric charging.

Corona Charging

Corona charging of powder works on the simple principle of subjecting a powder layer to a stream of ions. The ion beam is created by applying a high voltage on a thin 'corona' wire creating an ion cloud around the wire that is referred to as a 'corona'. The fundamental problem with corona charging of toner is that powder particles may be airborne in the developer and may then coat the corona wire, preventing it from being effective.

Injection Charging

Injection charging is a very straightforward method for charging a wide variety of non-conducting powders. The powder particles are exposed to a significant electric field. This is often accomplished by applying a voltage to a metallic foil attached to the doctor blade. The outer surface of the insulative toner material will take on charge as it is carried through the field. This is a very effective and popular means for powder charging, with the minor issue of requiring the use of a high voltage power source.

Triboelectric Charging

Triboelectric charging is used in most current-generation printers, often in conjunction with injection charging. When two dissimilar materials rub against each other they exchange charge causing both materials to become charged in opposite directions. This phenomenon is called triboelectric charging. The charge polarity as well as the amount of charge exchange depends on the two materials involved and therefore the material of the triboelectric surface must be chosen carefully. In large photocopiers, carrier particles are mixed in with toner to that these particles charge each other during mixing. Special charge control agents are often added to the toner powder to enhance triboelectric charging.

c) Powder Transport

The movement of powder from the hopper to the photoconductor drum is a very important and very difficult step in the development process. For proper imaging, a consistent layer of powder must be moved to the photoconductor drum without spilling. The doctor blade helps to maintain a consistent layer thickness so long as the transfer roller is initially bringing out a layer thicker than the doctor blade is designed to meter out. There are two main methods currently used for powder transport: magnetic and cascade transport.

Magnetic Transport

Magnetic transport is by far the most popular method for transporting powder. In this method, the toner particles are doped with a magnetic substance, usually an iron oxide compound, and the transport roller has a magnetic core that provides an attractive force for the particles. Either the magnetic core itself or an outer frictional roller revolves, circulating the powder with it. This method of transport virtually eliminates spilling, keeps powder flow consistent, and makes it fairly easy to predict the amount of powder the roller will draw out..

There is the added advantage that in the transfer stage, the particles must overcome the magnetic force by electric field force, which greatly reduces the transfer of wrong-sign charged toner. However, there is one notable disadvantage to this method, and that is the requirement of a magnetic material. In printing this means the method is only useful for magnetized powder, and the method is not favorable for ESFF because it introduces significant restrictions on the powder material.

Cascade Transport

Cascade transport is so named because in the very early days of electrophotography, images would be developed by pouring or "cascading" charged toner down a plate with a latent charge image. Toner would stick to the image areas due to electrostatic force, forming an image that could be transferred for permanent printing. In a modern system this process is a bit more complex. Toner is brought out of the hopper by mechanical force, usually friction, by a roller. A layer of the toner on the transfer roller then passes near the photoconductor drum, where particles are attracted to the properly charged areas. Because there is no adhesive force between the transfer roller and the toner, the doctor blade can knock off more powder than it is meant to meter, causing uneven prints. There are also unavoidable spilling problems.

This development method is necessary for color printing with electrophotography, but with ink-jet printers becoming comparably fast to laser printers the drawbacks of the system are preventing it from being used. This system is needed for ESFF because it can be used to develop arbitrary powders.

d) Powder Transfer

The final step of the development process is to transfer powder to the image on the photoconductor drum. The quality of this process in a given system is fundamentally a balance of forces. There is the electrostatic force pulling the charged particles towards the image, the adhesion forces to the surface to

which they are attached, and the attractive forces between particles. Ideally, there should be a strong tendency for particles to stay on the transfer roller due to adhesive forces except where drawn off by electrostatic effects. This produces a clear image with minimal transfer in the background areas.

This is easily accomplished in magnetic powder transport because of the strong magnetic attractive force. The charged powder is caused to jump on and off the roller by an AC field, creating a cloud of powder around the roller. The magnetic strength of the roller and the AC voltage can be varied to optimize printing. Cascade transport suffers more difficulties in this area since there is no strong attractive force to be overcome during development. For this reason, cascade systems will have significant background printing.

1.7.2. Evolution of ESFF developer design

In past work with the ESFF testbed, it has been necessary to use standard printer toner to build parts because of the lack of a system to print other powders. For reasons of construction simplicity and flexibility in terms of which powders would be printed, it was decided to use a design based on cascade transport and injection charging. This combination allows for development of nearly any non-conducting powder.

The first developer design, version 1.0, is shown in Figure 30. This design for the developer was a very simplistic device involving a powder hopper, a transfer roller, and a cantilevered doctor blade actuated by a screw plate. A press fit piece in one side allowed the roller to be removed laterally through a large opening. The roller itself pressed against the photoconductor drum directly. It was believed this would balance forces causing powder to adhere to the surfaces, leading to better development.

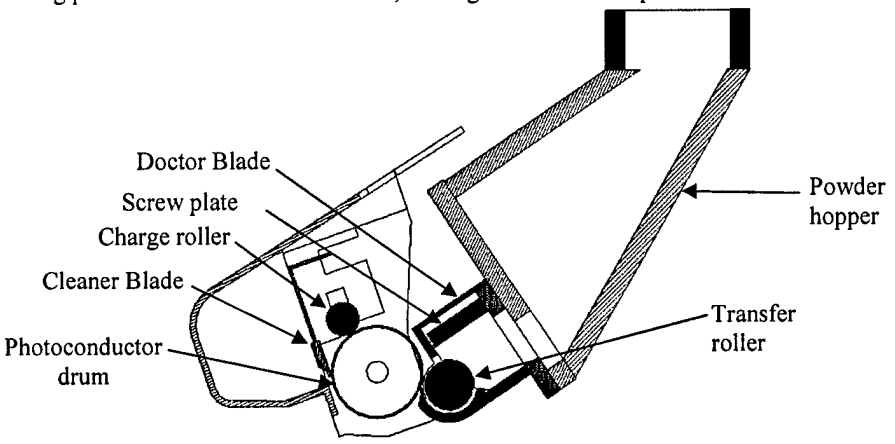

Figure 30: Cross-section of developer design, version 1

The charging ability of this powder was tested by measuring charge per unit mass of powder printed on the photoconductor. It was found that non-conducting powder was not charged efficiently resulting in poor prints. This design suffered from a number of other shortcomings. The plastic casing was not adequate to

prevent leaks. The doctor blade was not rigid enough to maintain a consistent powder flow across its length. Finally, the direct contact between the transfer roller and the photoconductor drum led to powder being sheared off, causing an unacceptable spillage rate. The bottom lip of the developer was also insufficient, because it sat too high and too close to the transfer roller to catch any powder which spilled off the bottom side of the roller.

Measures were taken to try and correct these problems within the context of the same basic design. The second design, version 2, of the developer is shown in Fig. 31. The plastic casing had foam gaskets added to reduce leaking. The roller was assembled by sliding it into narrow, baffled fittings. The bottom lip was brought as close as possible to the photoconductor drum to catch any falling powder. Offset rollers were added to provide a small gap between the transfer roller and the photoconductor drum, thus preventing spilling due to powder shear. The doctor blade was changed to a leaf-spring actuated design wherein powder would have to slide past the blade over a longer distance, leading to more consistency regardless of particle size. Also, small protrusions were added to the side of the casing which were meant to keep powder from reaching the side connections, further reducing leaking.

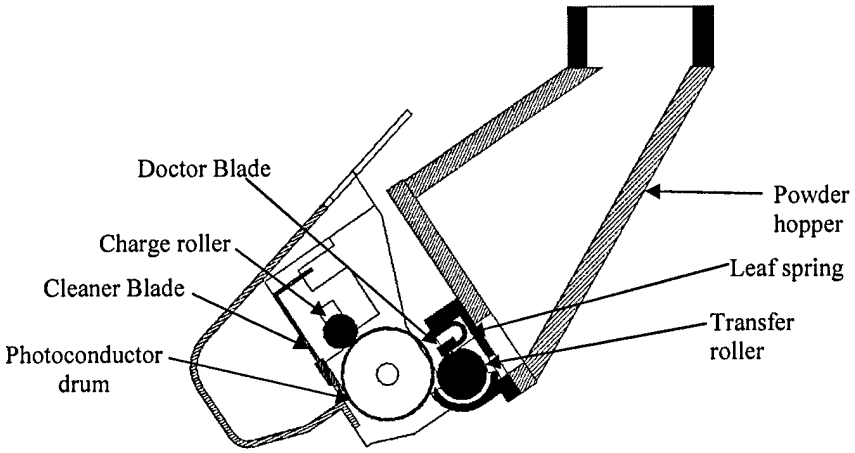

Figure 31: Cross section of improved developer design, version 2

By applying a voltage to the doctor blade, this developer was very effective in charging the powder. However, this design suffered from some of the same powder handling problems as the previous design, but showed improvement in many areas. Powder leaking from the casing itself was eliminated. The offset rollers used were not consistent enough in providing a uniform gap. The extended bottom lip was still not able to catch all powder falling from the transfer roller. The doctor blade had improved consistency, but was more difficult to actuate if a different flow rate was desired. The side protrusions added a great deal of friction, making the developer difficult to drive.

It was clear at this point that a different design path was needed. This resulted in another design, version 3, shown in Fig. 32. Successful ideas like gaskets and baffled fittings were kept and expanded, with almost all fittings now being baffled and gaskets added wherever desirable. A printing gap was included to prevent spilling due to shearing of powder in the printing interface. Instead of offset rollers, the gap in this system would be provided by tapes on a metal developer roller, providing a very thin and very consistent gap. A two-roller design was introduced, in hopes that by including an initial electrostatic transfer across a gap, the amount of powder brought out by the system could be reduced, and that the powder could then be effectively recirculated. It was also hoped this would give greater control over the charge density on the powder that would form the toner image.

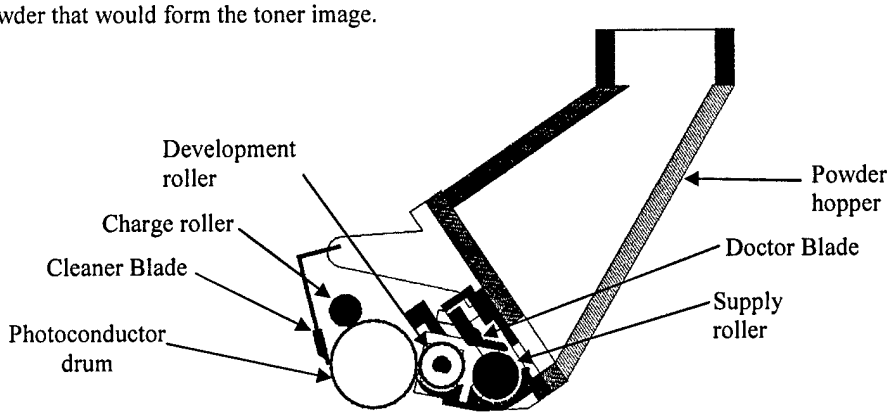

Figure 32: Cross-section of two-roller developer design, version 3

A pivoting doctor blade was used in this design to give better control over powder flow from the hopper. To achieve uniformity, precise control of the gap between the blade and the transfer roller is necessary, as are rigidity in the doctor blade and manufacturing tolerances. Powder is brought out of the hopper by a supply roller and is charged by the doctor blade and electrostatically transferred on to the development roller. The gap between the two rollers serves as a control over the charge density in the powder transferred to the development roller. The powder picked by the development roller is then transferred to the discharged areas of the photoconductor drum to create an image on the drum.

Like the previous design, this version was able to charge and print powder. Even though the powder leak problem was more or less eliminated, the powder printing was not very uniform. Too much powder printed in certain areas causing some of the excess powder to drop of the photoconductor after printing. This final design also greatly increased the complexity of the process. The doctor blade opening, the gaps between the two rollers and between the second roller and the photoconductor drum, and the charge voltage can all be varied. This is advantageous, in that it gives a great deal of control over the transfer process. However, there is a significant drawback in that these variables must be controlled precisely and consistently in order to maintain proper development.

The voltage applied to the doctor blade has two effects. It controls the amount of powder charge and it determines the electric field present between the photoconductor drum and the developer. A higher voltage will result in a higher average charge density in the toner. To maximize the mass transfer it is necessary to charge the powder to a critical threshold value, as too little charging will result in an inability to transfer, and too much charging will result in a small powder mass being adequate to cancel the field. Thus from the charging perspective, there is an optimal voltage. In establishing the overall field across the entire development process, it would be ideal to have an arbitrarily high voltage, since this will maximize the field and with it the mass of toner transferred.

The system was tested on a charge-measuring unit. The unit allows the testing of charge and mass, such that the performance of a particular toner powder can be measured and optimized. Some success was seen in charging and transferring powder. Preliminary testing with nylon powder showed that the device could transfer a powder layer across the printing gap onto a grounded drum after charging. This showed the capacity for electrophotographic development of an arbitrary non-conducting powder in its most basic form. The complexity of the design made manufacture and assembly difficult, leading for improper fits and uneven gaps.

The cascade developers were not tested in the ESFF testbed for part building due to leakage and non-uniform printing. However, the developers did yield many insights into the powder charging mechanism. Powder leakage could be ignored in charge measurement tests that allowed a systematic study of parameters that affect charging of powder. In the long run, a method for developing new powders is critical to the project. To overcome some of the problems associated with using the cascade developer it was decided that it is necessary to redesign the ESFF testbed as explained below.

1.8. Future directions

The experimental study showed the developers designed so far could charge a variety of powders. However, it was found that ensuring uniform powder flow and preventing leaks when the powder is not magnetic were two difficult issues. To overcome these difficulties, an entirely new architecture is necessary for the test bed. Figure 33 shows a schematic diagram of the proposed system. In this new configuration, a photoconducting plate will be used instead of a drum. A two-axis motion control system would be used, but instead of moving the build platform, the photoconductor plate is moved. The plate would move in the X direction (horizontal) during printing. It also needs to move in the Y direction to compensate for increasing part height on the build platform. The photoconductor plate would first move over a charging roller, to electrostatically charge its surface. Next it would pass over the imaging system where the charged surface is selectively discharged by the laser image scanner which scans the required image on to the plate. The regions where laser beam hits the photoconductor surface are discharged. Then the plate would move over the image developer, picking up powder on to the discharged areas of the photoconductor to form an image.

Multiple image developers can be used in this configuration, though only one at a time can be active. After the image has been formed on the photoconductor plate, the image will be transferred on to the build platform or over the previously printed layers. After transfer, the excess powder would be scraped off the plate using the cleaner and the plate would then return to begin another printing cycle.

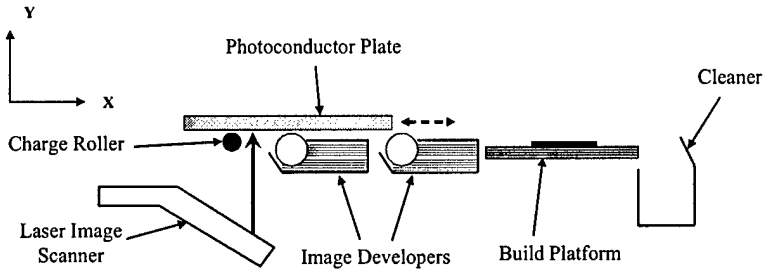

Figure 33: Conceptual schematic of the new ESFF testbed

In this new configuration for electrophotographic layered manufacturing, the developer would now print vertically upwards onto the photoconductor plate, instead of horizontally on a drum. This eliminates the problem of leakage of powder from the developer on to the part being built as in the previous design. In addition, the plate can pick up powder from multiple developers enabling multi-material layered manufacturing. Another advantage of this configuration is that it allows for translation of the photoconductor during the printing process (instead of rotation of a drum). This spreads out the various components of the printing system, making the design simpler as the components no longer need to be extremely compact.

The concept of the image developer shown in Fig. 33 has already been tested. It contains a conductive polyurethane development roller that brings out powder that sticks to the pores on its surface. A doctor blade is used to injection charge the powder sticking to this roller. An electrostatic field has to be created between the developing roller and the photoconductor plate to transfer the powder against gravity from the roller to the plate. In this developer, the powder is held to the developer roller by gravity in the same way magnetic force holds powder in the magnetic brush system.

The transfer of the imaged powder to the build platform could be accomplished by charge deposition on the part surface, as in the current system. Another method would be to repulse the powder using electrostatic force by applying a voltage to the photoconductor plate. A variety of methods for consolidation of powder will be explored. A heated compaction plate like the one currently used would serve the purpose for plastic parts. An ultrasonic bonding technique [33] or induction heating could enable

direct fusing of metal powders. It is also possible to selectively bind one or more of the printed powders using a liquid binder as in the case of 3D printer.

The laser image scanner, shown in Fig. 34, is a typically laser imaging system used in laser printers. It uses a laser diode to generate an ultraviolet laser beam to discharge the photoconductor. The laser is pulsed on and off to create a maximum resolution of 600 dots per inch. The laser beam is scanned back and forth as it is reflected by a polygonal mirror, which is rotated by a stepper motor.

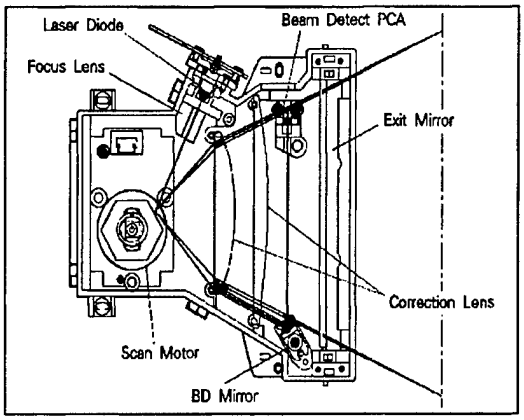

Figure 34: Laser image scanner

A laser printer has an image formatter which translates the print file, sent to it from a computer, into digital signals that drives the laser scanner. Since a laser printer is not being used in the new configuration for the layer manufacturing system, software needs to be developed to drive the laser scanner to print images of the cross-section of the part. This software has to generate dithered images to print in gray scale or some predetermined patterns within the cross-section image when necessary. This would allow us to print multiple powders in different gray scales to create composition variation within each layer rather just from one layer to the next. The ability to print multiple powders in layers in controlled fashion is necessary to realize the promise and potential of layered manufacturing systems to fabricate truly heterogeneous components, functionally gradient materials and products that cannot be manufactured by any other means.

1.9. Publications

Kumar Ashok V. and Dutta Anirban, "Investigation of an electrophotography based rapid prototyping technology", Rapid Prototyping Journal, vol. 9, issue 2, 2003, pp. 95-103.

Kumar, Ashok V. and Dutta Anirban, 2003, "Layered manufacturing by electrophotographic printing", Proceedings of DETC 2003, Design Automation Conference, ASME.

Kumar, Ashok V., Dutta Anirban and Fay James, 2003, "Solid freeform fabrication by electrophotographic printing", presented at 14th Solid Freeform Fabrication symposium, 2003 and accepted for publication in Rapid Prototyping Journal.

Kumar A. V. and Lee J., "Design and Slicing of Heterogeneous Components for Rapid Prototyping", 11th Solid Freeform Fabrication Proceedings, 2000.

Kumar A. V. and Wood A., "Representation and design of heterogeneous components", 10th Solid Freeform Fabrication Proceedings, pp. 179-186, 1999.

Kumar Ashok V. and Yu Lichao, "Sequential constraint imposition for dimension-driven solid models", *Computer Aided Design*, Elsevier Science, vol. 33, 2001, pp. 475-486.

Yu Lichao and Kumar Ashok V., "An object-oriented modular framework for implementing the Finite Element Method", *Computers and Structures*, Elsevier Science, vol. 79, 2001, pp. 919-928.

Kumar Ashok V., "A sequential optimization algorithm using logarithmic barriers: Applications to structural optimization", *Journal of Mechanical Design*, Transactions of the ASME, vol. 122, no. 3, 2000, pp. 271-277.

Kumar A. V. and Zhang H., "Electrophotographic powder deposition for freeform fabrication", 10th Solid Freeform Fabrication Proceedings, pp. 639-646, 1999.

Kumar, Ashok V., "Powder deposition and sintering for a two-powder approach to solid freeform fabrication", 9th Solid Freeform Fabrication symposium, 1998.

Kumar Ashok V., Patent Number: 6,066,285; Title: Solid freeform fabrication using powder deposition, Assignee: University of Florida, Gainesville, FL; Date filed: December 11, 1998.

1.10. References

[1] Kumar A. V. and Zhang H., "Electrophotographic powder deposition for freeform fabrication", 10th Solid Freeform Fabrication Proceedings, pp. 639-646, 1999.

[2] Kumar, Ashok V., Dutta Anirban and Fay James, 2003, "Solid freeform fabrication by electrophotographic printing", presented at 14th Solid Freeform Fabrication symposium, 2003 and accepted for publication in Rapid Prototyping Journal.

[3] Kumar, Ashok V. and Dutta Anirban, 2003, "Layered manufacturing by electrophotographic printing", Proceedings of DETC 2003, Design Automation Conference, ASME.

[4] Kumar Ashok V. and Dutta Anirban, "Investigation of an electrophotography based rapid prototyping technology", Rapid Prototyping Journal, vol. 9, issue 2, 2003, pp. 95-103.

[5] Kumar Ashok V., Patent Number: 6,066,285; Title: Solid freeform fabrication using powder deposition, Assignee: University of Florida, Gainesville, FL; Date filed: December 11, 1998.

[6] Schien L., B., "Electrophotography and Development Physics", Springer-Verlag, NY, 1988

[7] Cross, J. A., "Electrostatics Principles, Problems and Applications," pp. 48-49, Adam Hilger, Bristol, 1987.

[8] Keithley Manual, 6517A Electrometer.

[9] Gao Y. and Doumanidis C., "Mechanical analysis of ultrasonic bonding for Rapid Prototyping", Journal of Manufacturing Science and Engineering, vol 124, pp.426-435, 2002.